Revista Mexicana de Astronomía y Astrofísica, **40**, 69–79 (2004)

STRUCTURAL PROPERTIES OF SPHERICAL GALAXIES: A SEMI-ANALYTICAL APPROACH

E. Simonneau

Institut de Astrophysique de Paris, CNRS, France

F. Prada[1]

Instituto de Astrofísica de Andalucía (CSIC), Spain

Received 2002 February 25; accepted 2004 February 18

RESUMEN

Puesto que la distribución de luz medida sobre cualquier radio galactocéntrico de una galaxia elíptica tiene la misma forma funcional: $exp[-R^{1/n}]$ (perfil de Sérsic) para casi todas estas galaxias, y dado que este perfil es la integral de Abel de la densidad espacial de fuentes luminosas $\rho_L(r)$, parece lógico buscar el camino de derivar esta densidad a partir de la distribución de luz observada. Proponemos en este artíiculo un método de "ordenadas discretas" que proporciona, para cualquier $n > 1$, una expresión explícita para esa densidad de fuentes emisoras, tal que puede evaluarse numéricamente con cualquier grado de precisión. Una vez obtenida esa densidad $\rho_L(r)$, se calculan fácilmente la distribución de masa $M(r)$, el potencial $\phi(r)$ y la dispersión de velocidades, tanto en el espacio $\sigma_s^2(r)$ como en el plano de observación, $\sigma_p^2(R)$.

ABSTRACT

Since the distribution of light measured along any galactocentric radius of an elliptical galaxy has the same functional form $exp[-R^{1/n}]$ (Sérsic profile) for almost all galaxies, and since this profile is the Abel integral of the luminous density, it looks worth-while to seek the way to derive the latter from the former. We propose in this paper a "discrete ordinate" method, which yields, for any value of $n > 1$, an explicit expression for the luminous density, $\rho_L(r)$, that can be evaluated numerically to any required degree of precision. Once we have obtained such an expresion for the spatial density, $\rho_L(r)$, we can compute straightforwardly the mass distribution, $M(r)$, the potential, $\phi(r)$, and the velocity dispersions, $\sigma_s^2(r)$, in space and on the observational plane, $\sigma_p^2(R)$.

Key Words: **GALAXIES: ELLIPTICAL — GALAXIES: KINEMATICS AND DYNAMICS — GALAXIES: STRUCTURE**

1. INTRODUCTION

The analysis of the light intensity distribution over the surface of an elliptical galaxy is fundamental in order to determine its internal structure. Already the first studies pointed out that this intensity distribution along a galactocentric radius is similar for all galaxies, and this holds true also for the bulges of spiral galaxies. This distribution was first represented by the Hubble-Reynolds law $I(R) \propto (R + R_o)^{-2}$ (Reynolds 1913; Hubble 1930), and some time later by the "universal" $R^{1/4}$ de Vaucouleurs law (de Vaucouleurs 1948). However, subsequent observations (Davies et al. 1988; Caon, Capaccioli, & D'Onofrio 1993; Andreakis, Peletier, & Balcells 1995; Graham et al. (1996); Binggeli & Jergen 1998) have shown some discrepancies with the $R^{1/4}$ law, leading to a more general form $R^{1/n}$, usually with $n > 1$ (Sérsic 1968). This three-parameter expression accounts much better for the observed intensity profiles of both elliptical galaxies and bulges of spiral galaxies.

In this paper we present an exhaustive study to determine the 3D spatial distribution of emitting sources from any observed $R^{1/n}$ Sérsic profile. Then, via a mass-to-luminosity ratio, we are able to derive the corresponding dynamical properties.

[1] Ramón y Cajal Fellow, Spain.

2. THE ABEL INVERSION FOR THE SERSIC PROFILES

For an spherical galaxy of total luminosity L, the "light profile", which describes the light intensity distribution along any galactocentric radius, can be approximated by the Sérsic profile

$$I(R) = I(0)\exp[-k(R/R_{\rm e})^{\frac{1}{n}}] \quad . \tag{1}$$

Then, the luminosity L is given by

$$L = I(0)R_e^2\pi\frac{2n}{k^{2n}}\Gamma(2n) \quad , \tag{2}$$

where $\Gamma(2n)$ is the Gamma function. R_e is the effective radius, i.e., the "radius" of the isophote that encloses one half of the total luminosity. For $n \geq 1$, k can be estimated (with an error smaller than 0.1%) by the relation $k = 2n - 0.324$ (see Ciotti 1991).

Our aim is to determine the density of galactic luminous sources which can explain the observed intensity profile, $I(R)$, given by Eq. (1). This intensity at a given position is due to the emission of all the stars lying on the line of sight. In the case where the emitting sources of the galaxy have a spherical distribution of density, $\rho_L(r)$, the observed isophotes should be circular, and the corresponding intensity will be given by

$$I(R) = \int_R^\infty \rho_L(r)\frac{2r{\rm d}r}{\sqrt{r^2-R^2}}, \tag{3}$$

where R is the radius of each observed isophote.

If the distribution of emitting sources is not spherical, as it happens in the case of actual elliptical galaxies, the relation between the observed intensity profile I and the spatial distribution of luminous sources ρ is, in practice, the same (Lindblad 1956; Stark 1977). In this paper, then, we shall consider only the case of spherical galaxies by means of Equation (3). But we would like to emphasize that many of the conclusions presented in this paper can be applied, with minor changes, to the case of elliptical galaxies.

Thus, in terms of the new variables $z \equiv (R/R_e)$ and $s \equiv (r/R_e)$, the theoretical inversion of the Abel integral transform (Tricomi 1985; Binney & Tremaine 1987), can be writen in the form

$$R_e\rho_L(s) = -\frac{1}{\pi}\int_s^\infty \frac{{\rm d}I(z)}{{\rm d}z}\frac{{\rm d}z}{\sqrt{z^2-s^2}}, \tag{4}$$

where $I(z)$ is given by the Eq. (1). Thus, it follows that

$$\rho_L(s) = \frac{1}{\pi}\frac{k}{n}\frac{I(0)}{R_e}\int_s^\infty \frac{\exp[-kz^{\frac{1}{n}}]\,z^{\frac{1}{n}-1}}{\sqrt{z^2-s^2}}{\rm d}z, \tag{5}$$

or, alternatively (for $n \geq 1$) with $z = t^n s$

$$\rho_L(s) = \frac{k}{\pi}\frac{I(0)}{R_e}s^{\frac{1}{n}-1}\int_1^\infty \frac{\exp[-ks^{\frac{1}{n}}t]}{\sqrt{t^{2n}-1}}{\rm d}t. \tag{6}$$

Of course the divergence of $\rho_L(s)$ for $s = 0$ is a direct consequence of the form of the empirical Sérsic law used to describe the observed $I(R)$. However, this a minor problem because the corresponding mass distribution, Eq. (19) does not present any discontinuity.

Although the argument in the integral of Eq. (6) is singular at $t = 1$, it is integrable for any value of n.

When $n = 1$ the intensity profile, $I(R)$, takes the form of an exponential law and the integral in Eq. (6) is the $K_o(x)$ modified Bessel function, which has a logarithmic discontinuity for $x = 0$ (see Abramowitz & Stegun 1964, pages 374–376). Hence, for $n = 1$ the spatial density becomes

$$\rho_L(s) = \frac{k}{\pi}\frac{I(0)}{R_e}K_o(ks). \tag{7}$$

For $n > 1$ the integration of Eq. (6) is not possible analytically. However, for $s = 0$ it holds that

$$\int_1^\infty \frac{{\rm d}t}{\sqrt{t^{2n}-1}} = \frac{1}{2n}B(\frac{1}{2},\frac{n-1}{2n}) \tag{8}$$

However, the form of the integral in Eq. (6) has been used by many authors to obtain different approximations for $\rho_L(s)$. First, for the de Vaucouleurs case $n = 4$, by Poveda, Iturriaga, & Orozco (1960), Mellier & Mathez (1987); subsequently for the Sérsic profiles by Gerbal et al. 1997. Also, numerical computations of $\rho_L(s)$ have been carried out by Young (1976) for the de Vaucouleurs case and by Ciotti (1991) and Graham & Colles (1997) for the Sérsic cases, respectively. In this article we propose an analytical approximation for $\rho_L(s)$ that makes possible an easy computation of the mass and gravitational potential to any required degree of precision.

As the argument of the integral in Eq. (6) can be integrated for any value of s, irrespectively of the singularity at $t = 1$, it seems possible to rewrite this integral in the variable, x, such that the argument does not show any discontinuity. Our choice is $t = 1/(1-x^2)^{1/(n-1)}$. Eq. (6) for the density becomes then

$$\begin{aligned}\rho_L(s) \quad &= \quad \frac{k}{\pi}\frac{I(0)}{R_e}\frac{2}{n-1}\frac{1}{s^{\frac{n-1}{n}}} \\ &\int_0^1 \frac{\exp[-ks^{\frac{1}{n}}(1-x^2)^{-\frac{1}{n-1}}]}{\sqrt{1-(1-x^2)^{\frac{2n}{n-1}}}}\,x{\rm d}x. \end{aligned} \tag{9}$$

TABLE 1

ABSCISSAE, x_j, AND WEIGHTS, w_j[a]

	x_j	w_j
$N_{ap} = 1$	0.5	1.
$N_{ap} = 2$	0.211325	0.5
	0.788675	0.5
$N_{ap} = 5$	0.046910	0.118464
	0.230765	0.239314
	0.5	0.284444
	0.769235	0.239314
	0.953090	0.118464

[a]For the Gaussian integration in the interval (0,1) for three different approximations, N_{ap}=1,2 and 5.

We can now formally perform the integration by means of a Gaussian numerical integration to obtain

$$\rho_L(s) = \frac{k}{\pi}\frac{I(0)}{R_e}\frac{2}{n-1}\frac{1}{s^{\frac{n-1}{n}}}\sum_{j=1}^{N_{ap}}\rho_j \exp[-\lambda_j k s^{\frac{1}{n}}] \quad , \tag{10}$$

where

$$\lambda_j = \frac{1}{(1-x_j^2)^{\frac{1}{n-1}}} \quad , \tag{11}$$

$$\rho_j = w_j \frac{x_j}{\sqrt{1-(1-x_j^2)^{\frac{2n}{n-1}}}} \quad , \tag{12}$$

and x_j and w_j ($j = 1, 2, ..., N_{ap}$) are respectively the Gaussian abcissae and the corresponding integration weights with the interval $(0, 1)$. N_{ap} is the order of approximation, i.e., number of abscissae and weights necessary to evaluate numerically the integral in Eq. (6). In Table 1 we have listed the abscissae and weights for the $N_{ap} = 1, 2$ and 5 cases that we discuss below.

The standard tables of abcissae, $\bar{x}_j$, and integration weights, $\bar{w}_j$, correspond to the interval $(-1, +1)$ (Abramowitz & Stegun 1964, pages 916–919). Therefore, the relation of the values of x_j and w_j for the interval (0,1) are $x_j = (1 + \bar{x}_j)/2$ and w_j=$\bar{w}_j/2$.

Now, in order to test the quality of our approximations, we shall start by pointing out that there are a few characteristic quantities relevant to the distribution $\rho_L(s)$ that can be determined independently of the numerical approximations. These quantities enable us to perform a first check of our approximate form for $\rho_L(s)$ in Eq. (10). One of them is the integral in Eq. (8) which determines the asymptotical behaviour of $\rho_L(s)$ when $s \to 0$. From Eqs. (8) and (10) it is necessary that

$$\frac{4n}{n-1}\sum_{j=1}^{N_{ap}}\rho_j \sim B(\frac{1}{2}, \frac{n-1}{2n}), \tag{13}$$

where the coefficients ρ_j are those given by Eq. (12). The other characteristic quantities are the different moments of the density distribution, $\rho_L(r)$, defined by

$$M\rho_m = \int_0^\infty \rho(r) r^m \mathrm{d}r = \frac{1}{B(\frac{m}{2}, \frac{1}{2})} MI_m, \tag{14}$$

where $B(z, w)$ is the complete Beta (Euler) function, and MI_m are the moments of the observed intensity given by

$$MI_m = \int_0^\infty I(R) R^{m-1} \mathrm{d}R = R_e^m I(0) \frac{n}{k^{nm}} \Gamma(nm). \tag{15}$$

The first one ($m = 0$) leads to the synthetic value of $I(0)$. To satisfy Eq. (3) for $R = 0$ with a density law as in Eq. (10) it is necessary that

$$\sum_{j=1}^{N_{ap}} \frac{\rho_j}{\lambda_j} \sim \frac{\pi}{2}\frac{n-1}{2n}. \tag{16}$$

The second one ($m = 1$) leads to the value of the gravitational potential at the centre of the system ($r = 0$). This value, $\phi(0)$, is known a priori; it is obtained directly from the analytical solution of the Poisson equation in the center, $s = 0$ (see below Eq. [21]). To reach this theoretical value with a density law as in Eq. (10) is necessary that

$$\sum_{j=1}^{N_{ap}} \frac{\rho_j}{\lambda_j^{n+1}} \sim \frac{n-1}{2n}. \tag{17}$$

The third one ($m = 2$) leads to the value of the total luminosity, L. To have the same theoretical value as in Eq. (2) it is necessary that

$$\sum_{j=1}^{N_{ap}} \frac{\rho_j}{\lambda_j^{2n+1}} \sim \frac{\pi}{4}\frac{n-1}{2n}. \tag{18}$$

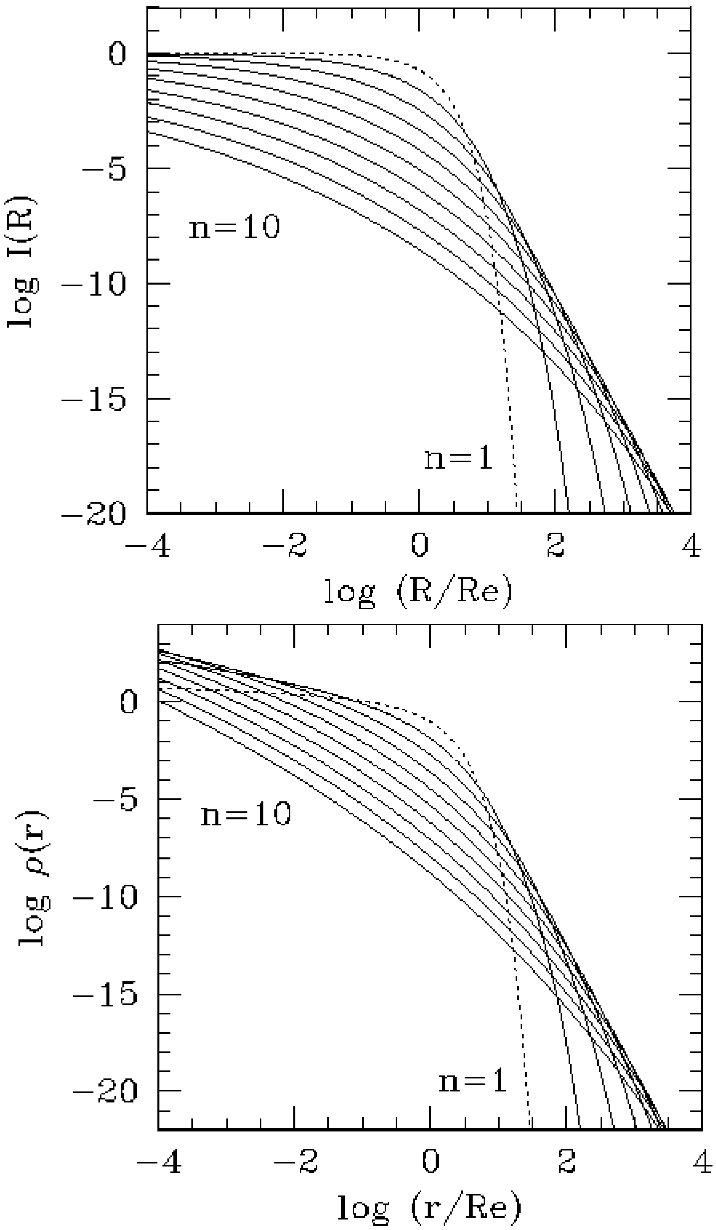

Fig. 1. *Top*: the surface distribution of intensity, $I(R)$ normalized to $I(0)$; this is Sérsic law for different values of the exponent n ($n = 1, 2, ..., 10$) in Eq. (1). R_e is the effective radius of the corresponding galaxy. The dotted line correspond to $n = 1$. *Bottom*: the corresponding density of luminous sources $\rho(r)$ given by equation (10), in units of $I(0)/R_e$.

Thus, to test as a first step the accuracy of our approximation for $\rho_L(s)$ in Eq. (10), we have computed the left-hand side of Eqs. (13), (16), (17), and (18) numerically; and in Tables 2, 3, 4, and 5 we have compared these with the theoretical values of their right-hand sides for the different approximations N_{ap} =1, 2, and 5, and for different values of n (2, 3,4 ,..., 10). As can be seen, the approximation $N_{ap} = 5$ leads to results of high quality. According to the results we have that for $N_{ap} = 10$, 20, and 40, the variation is insignificant with respect to the results for $N_{ap} = 5$.

We shall now discuss the accuracy of each approximation for $\rho_L(s)$ (N_{ap} =1, 2, 5, 10, 20, 40) over the entire interval. As a reference we take the density $\rho_{40}(s)$ calculated with $N_{ap} = 40$. The relative variation between this one and $\rho_{20}(s)$, calculated with the approximation $N_{ap} = 20$, is always smaller

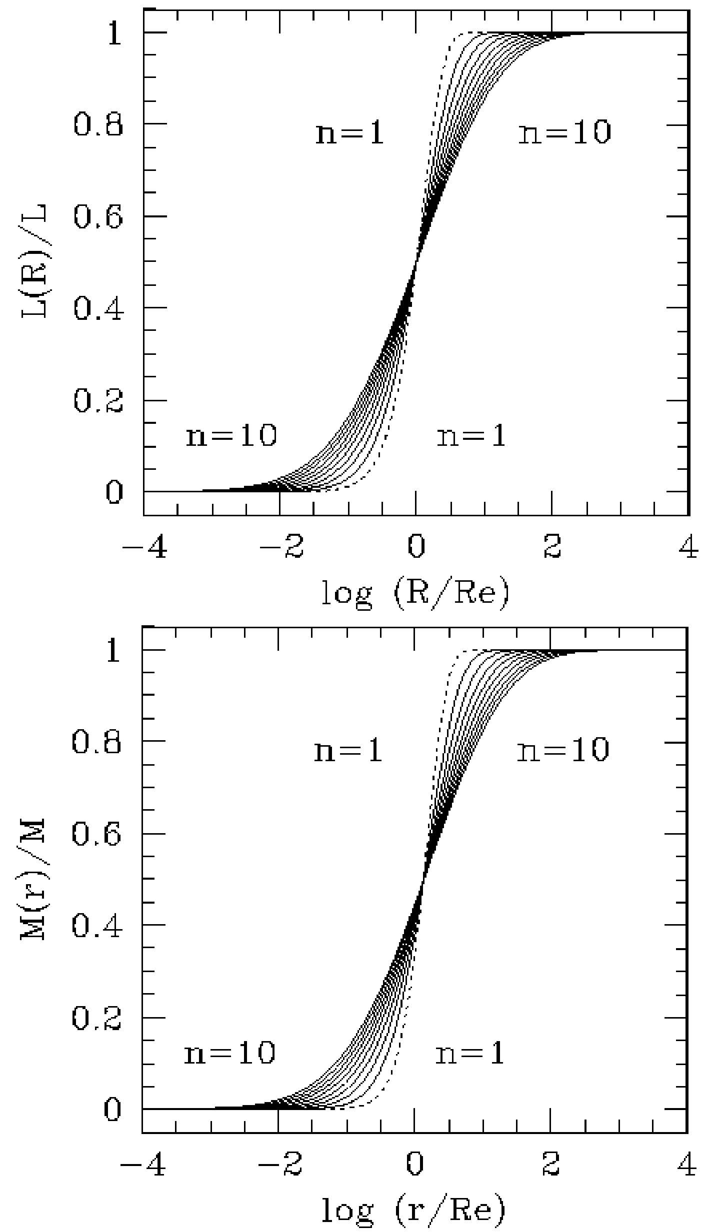

Fig. 2. *Top*: plot of the normalized luminosity distribution $L(r)/L$ corresponding to the $I(R)$ Sérsic profiles for $n = 1, 2, ..., 10$. *Bottom*: plot of the normalized mass $M(r)/M$ for the same values of n.

than 0.01%, i.e., negligible to the first four significant figures. This difference increases by one order of magnitude for the approximation with $N_{ap} = 10$. The relative difference between $\rho_{10}(s)$ and $\rho_{40}(s)$ is always smaller than 0.1%. For the case with $N_{ap} = 5$ the difference between $\rho_5(s)$ and $\rho_{40}(s)$ is always less than 1%. For the case of $N_{ap} = 2$ we can get differences of around 10% only for low values of n (less that 5), and for large values of s (greater than 10). This relative difference increases significantly for $N_{ap} = 1$. Thus, if we consider as not significative the difference between the cases with $N_{ap} = 40$ and $N_{ap} = 20$, we can take the above difference as the error of any approximation. In general, $N_{ap} = 2$ is a good approximation for a suitable first-order description.

Then, for most applications, when great accuracy is not necessary, the approximation $N_{ap} = 5$ can be sufficient. In case a much higher accuracy is required, the $N_{ap} = 10$ and $N_{ap} = 20$ approxima-

TABLE 2

ASYMPTOTIC VALUE OF ρ_L(s) FOR s $\to 0$, Eq. (8) [a]

n	(1)	$N_{ap}=1$	$N_{ap}=2$	$N_{ap}=5$
2	5.2441151	4.837945	5.255770	5.244083
3	4.2065460	3.945576	4.204081	4.206550
4	3.8558066	3.643523	3.850307	3.855832
5	3.6790940	3.490923	3.672538	3.679124
6	3.5725536	3.398728	3.565529	3.572583
7	3.5012896	3.336962	3.494024	3.501318
8	3.4502622	3.292684	3.442860	3.450289
9	3.4119198	3.259382	3.404436	3.411943
10	3.3820539	3.233423	3.374518	3.382076

[a](1). We show the exact value of $B(1/2,(n-1)/2n)$ and the corresponding computed values $\frac{4n}{n-1}\sum_{j=1}^{N_{ap}}\rho_j$, Eq. (13), with N_{ap}=1, 2, 5.

TABLE 3

SYNTHESIS OF THE OBSERVED CENTRAL INTENSITY $I(0)$ [a]

n	(1)	$N_{ap}=1$	$N_{ap}=2$	$N_{ap}=5$
2	0.3926991	0.453557	0.397601	0.392702
3	0.5235988	0.569495	0.537842	0.524518
4	0.5890502	0.620693	0.603678	0.590514
5	0.6283185	0.649734	0.641712	0.629974
6	0.6544985	0.668478	0.666468	0.656182
7	0.6731984	0.681587	0.683865	0.674842
8	0.6872234	0.691273	0.696759	0.688799
9	0.6981317	0.698723	0.706698	0.699631
10	0.7068726	0.704633	0.714593	0.708280

[a](1). We show the theoretical value of $(\pi/2,(n-1)/2n)$ together with the corresponding numerical computation of $\sum_{j=1}^{N_{ap}}\rho_j/\lambda_j$, Eq. (16), with N_{ap} =1, 2, 5.

tions can be good enough.

In Figure 1, we plot $\rho_L(r)$ as a function of $s=r/R_e$, for different values of n, together with $I(R)$ so as to exhibit the small, but representative differences between the two functions related by the Abel transform.

3. DYNAMICAL INFERENCES

Once we have obtained the density of luminous sources, $\rho_L(s)$, we can study some other quantities related to the dynamical state of the galaxy.

The density $\rho_L(s)$ in Eq. (10) refers to the density of luminous sources. In cases where the mass-to-luminosity ratio, Υ, is the same throughout the galaxy, the corresponding mass distribution, M, will be given by

$$\frac{M(s)}{M} = \frac{4}{\pi(n-1)\Gamma(2n)} \sum_{j=1}^{N_{ap}} \frac{\rho_j}{\lambda_j^{2n+1}}\gamma(2n+1,\lambda_j k s^{\frac{1}{n}}), \quad (19)$$

where $\gamma(2n+1,\lambda_j k s^{\frac{1}{n}})$ is the incomplete Gamma function corresponding to the Gamma function $\Gamma(2n+1)$ for the value $\lambda_j k s^{\frac{1}{n}}$. For $n=1$ the distribution of mass must be computed directly from the corresponding density given by Eq. (7). The total mass M is given as a function of the total luminosity, given by Eq. (2), multiplied by the factor Υ.

Because the Gaussian values of λ_j and ρ_j satisfy Equation (18) very accurately we are sure about the correct normalization in the $M(s)$ distribution. The normalized mass distribution, $M(s)/M$, is shown in Figure 2 for different values of n. We show in the same figure the normalized luminosity distribution $L(R)/L$.

Now, for the gravitational potential we have

$$\phi(s) = \frac{2n\phi(0)}{(n-1)\Gamma(n+1)} \sum_{j=1}^{N_{ap}} \frac{\rho_j}{\lambda_j^{n+1}}\gamma(n+1,\lambda_j k s^{\frac{1}{n}}) + - (\frac{\Upsilon G L}{R_e})\frac{1}{s}\frac{M(s)}{M} \quad , \quad (20)$$

where $M(s)/M$ is given by Eq. (19) and where the potential at the center is given by

$$\phi(0) = -(\frac{\Upsilon G L}{R_e})\frac{2}{\pi}k^n\frac{\Gamma(n)}{\Gamma(2n)} \quad , \quad (21)$$

which is the correct value known a priori (see Ciotti 1991). The fact that the Gaussian values of λ_j and ρ_j account for the first moments of the density law assures the correct normalization of the $M(s)$ and $\phi(s)$ distributions.

Curves for the potential $\phi(s)$ for different values of n ($n=1,2,...,10$) are shown in Figure 3.

With the above expressions for $\rho(s)$, $M(s)$ and $\phi(s)$ it becomes very easy to compute the total potential energy

$$W = \frac{1}{2}\int_0^\infty 4\pi r^2\rho(r)\phi(r)\mathrm{d}r, \quad (22)$$

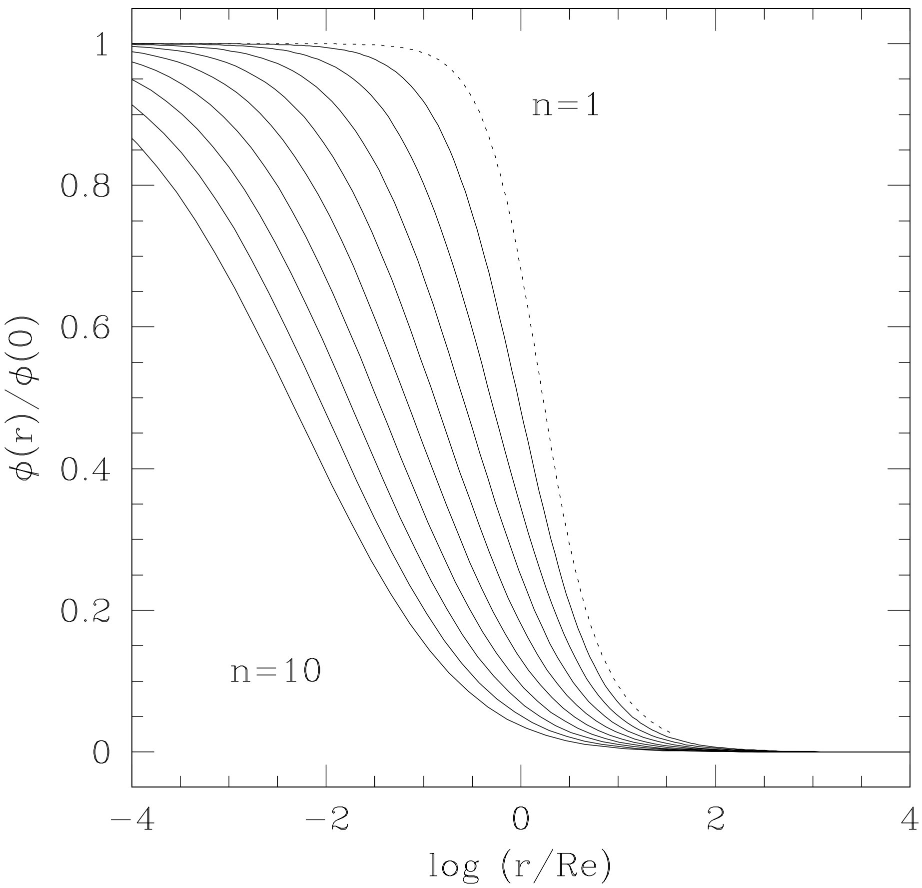

Fig. 3. Curves for the normalized potential $\phi(s)/\phi(0)$ for $n = 1, 2, ..., 10$.

to get

$$-W = \Upsilon^2 \frac{GL^2}{R_e} w^2. \tag{23}$$

The values of the parameter w^2, defined from Eq. (23), have been computed numerically and are given in Table 6 for the different values of n.

3.1. *The Velocity Dispersion*

We can interpret the term $(\Upsilon \mathrm{GL}/R_e)w^2$, as a mean quadratic velocity such that the corresponding kinetic energy, $T = (1/2)M(\Upsilon \mathrm{GL}/R_e)w^2$, satisfies the virial theorem. In spherical galaxies, this mean quadratic velocity —mean square of the space (3-D) stellar velocities— must correspond to the mean quadratic velocity dispersion $<\sigma^2(r)>$, where $\sigma^2(r) = {\sigma_x}^2(r) + {\sigma_y}^2(r) + {\sigma_z}^2(r)$. Then, in stationary spherical galaxies we can assume that there are no organized motions of the stellar populations as a whole; we can also assume the isotropy condition in the velocity dispersion tensor: ${\sigma_x}^2(r) = {\sigma_y}^2(r) = {\sigma_z}^2(r) = {\sigma_s}^2(r)$. Under this condition it holds that $<\sigma^2(r)> = 3 <{\sigma_s}^2(r)> = 3{\sigma_s}^2$.

If observations of the above mean quadratic velocity (velocity dispersion), independent of the observations of the profile $I(R)$, were available, under the assumption of the validity of the "Sérsic model" for the galaxy we could derive the potential energy from any observed $I(R)$ profile (cf. Eq. [22]), and consequently the factor w^2. Hence, we could estimate the value of the mass-to-luminosity ratio Υ from the virial theorem. This method for the determination of the masses of elliptical galaxies was proposed by Poveda (1958) for the case $n = 4$ (de Vaucouleurs law).

However, we cannot actually measure the velocity dispersion in space, $\sigma_s(r)$. We can measure only its "projection" on the observational plane, the so-called velocity dispersion on the observational plane, $\sigma_p(R)$. Theoretically, these measurements can be represented by

$$I(R)\sigma_p^2(R) = \int_R^\infty \sigma_s^2(r)\rho_L(r)\frac{2r}{\sqrt{r^2 - R^2}}dr, \tag{24}$$

which corresponds to the integral along the line of

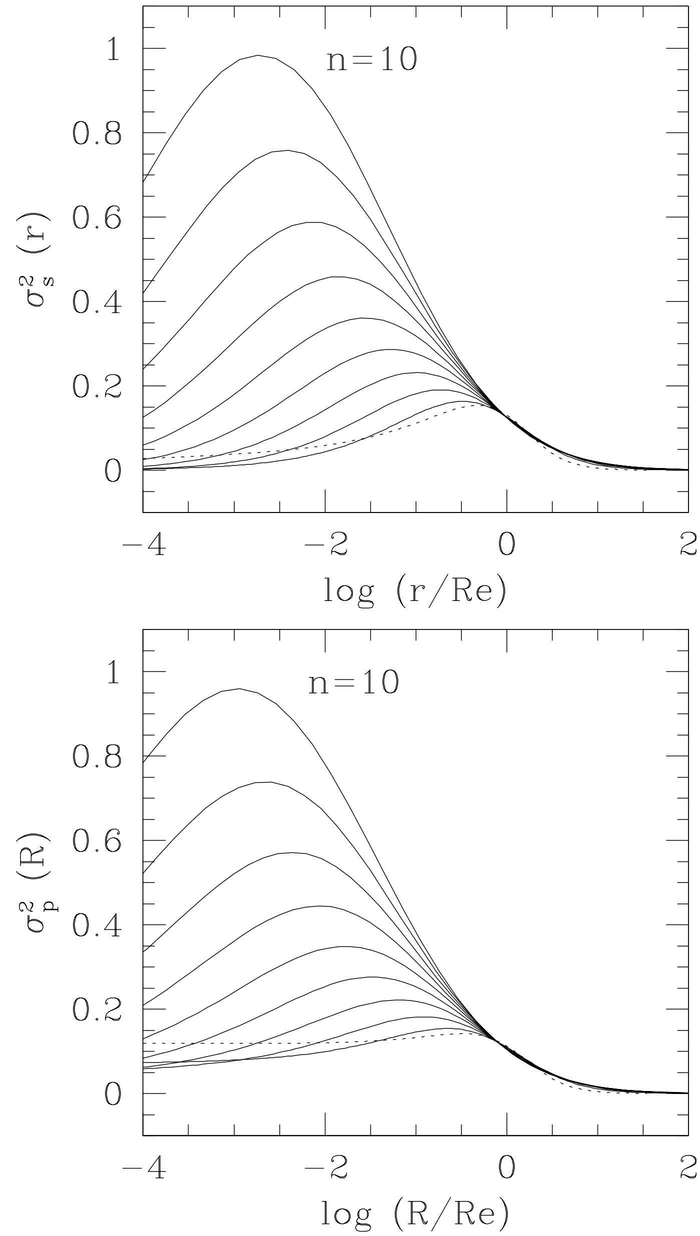

Fig. 4. *Top*: plot of the spatial velocity dispersion $\sigma_s^2(r)$ derived from Eq. (28) for $n = 1, 2, ..., 10$. *Bottom*: plot of the observed velocity dispersion $\sigma_p^2(R)$ derived from Eq. (24) for the same values of n. $\sigma_s^2(r)$ and $\sigma_p^2(R)$ are normalized to GM/R_e.

sight of the line-of-sight component of the spatial velocity the dispersion, i.e., $\sigma_s^2(r)$ weighted by the density of light. The mean quadratic value of $\sigma_p^2(R)$ is

$$< \sigma_p^2(R) >= \frac{\int_0^\infty \sigma_p^2(R) dL(R)}{L} = \sigma_p^2. \qquad (25)$$

On the other hand, the mean quadratic space velocity dispersion is given by

$$< \sigma^2(r) >= 3\frac{\int_0^\infty \sigma_s^2(r) r^2 \rho(r) dr}{\int_0^\infty r^2 \rho(r) dr} = 3\sigma_s^2 \quad . \qquad (26)$$

Equations (23) to (25), together with the defini-

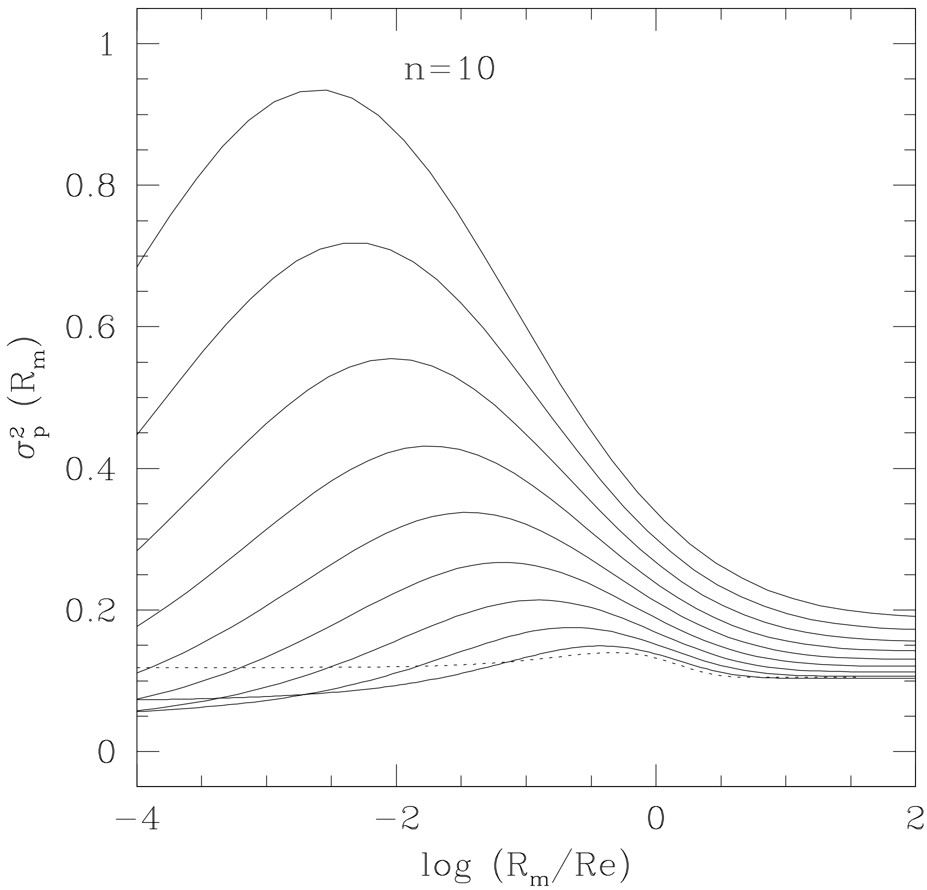

Fig. 5. Plot of the aperture velocity dispersion $\sigma_p^2(R_m)$, normalized to GM/R_e, derived from equation (29) for different values of the exponent n ($n = 1, 2, ..., 10$) in the Sérsic profile.

tion of $I(R)$ given by Eq. (1), assure that the condition $\sigma_p^2 = \sigma_s^2$ is satisfied. This offers us a way to estimate the mean quadratic spatial velocity dispersion, $3\sigma_s^2$, and, via the virial theorem, the mass-to-luminosity ratio, Υ.

But the measurement of the velocity dispersion averaged over the observation plane, Eq. (25), requires an integration over the entire image of the galaxy, namely, from the mathematical standpoint, over the entire radial interval from $0 < R < \infty$. In general, this condition cannot be satisfied and we can measure only $I(R)\sigma_p^2(R)$ over a radial interval $(0, R_m)$ which does not contain the entire luminosity L of the galaxy. This can lead to an incorrect value of σ_p^2, and therefore a wrong estimate of the mass-to-luminosity ratio, Υ, from the virial theorem.

However, this lack of spatial coverage in the observations can be compensated thanks to our galaxy model. Once we have the density distribution law, Eq. (12), and the potential distribution, Eq. (20), the spatial velocity dispersion, $\sigma_s^2(r)$ (assuming isotropy in the velocity distribution function), satisfies the Maxwell–Jeans equation,

$$\frac{d}{dr}\rho(r)3\sigma_s^2(r) = -\rho(r)\frac{d}{dr}\phi(r), \qquad (27)$$

and, with the natural boundary condition $\rho(r)\sigma_s^2(r) \to 0$ for $r \to \infty$, we have

$$\begin{aligned} \rho(r)3\sigma_s^2(r) &= \int_r^\infty \rho(r')\frac{d}{dr'}\phi(r')dr' \\ &= G\int_r^\infty \rho(r')\frac{M(r')}{r'^2}dr' \quad . \qquad (28) \end{aligned}$$

Equations (10) for $\rho(r)$ and (19) for $M(r)$ allow the direct calculation of $\sigma_s^2(r)$ from $r = 0$ to $r = \infty$. Afterwards, we can use Eq. (24) to get, via our model, the local mean velocity dispersion, $\sigma_p^2(R)$, on the observational plane.

TABLE 4

SYNTHESIS OF THE THEORETICAL GRAVITATIONAL POTENTIAL AT $S = 0$ [a]

n	(1)	$N_{ap} = 1$	$N_{ap} = 2$	$N_{ap} = 5$
2	0.25	0.255126	0.246949	0.249997
3	0.3333333	0.369898	0.327389	0.333356
4	0.375	0.422952	0.370122	0.374965
5	0.4	0.453484	0.396269	0.399942
6	0.4166667	0.473327	0.413849	0.416597
7	0.4285714	0.487259	0.426461	0.428498
8	0.4375	0.497580	0.435943	0.437496
9	0.4444444	0.505533	0.443330	0.444371
10	0.45	0.511849	0.449245	0.449928

[a](1) We show the theoretical value of $(n-1)/2n$ together with the corresponding numerical computation of $\sum_{j=1}^{N_{ap}} \rho_j/\lambda_j^{n+1}$, Eq. (17), with N_{ap}=1,2,5.

TABLE 5

SYNTHESIS OF THE THEORETICAL VALUE OF THE TOTAL LUMINOSITY [a]

n	(1)	$N_{ap} = 1$	$N_{ap} = 2$	$N_{ap} = 5$
2	0.1963495	0.143508	0.208820	0.196357
3	0.2617994	0.240256	0.265076	0.261793
4	0.2945431	0.288208	0.294168	0.294525
5	0.3141592	0.316511	0.312086	0.314166
6	0.3272492	0.335146	0.324230	0.327259
7	0.3365992	0.348335	0.333001	0.336611
8	0.3436117	0.358159	0.339631	0.343623
9	0.3490659	0.365757	0.344818	0.349077
10	0.3534292	0.371810	0.348987	0.353441

[a](1) We show the theoretical value of $(\pi/2, (n-1)/2n)$ together with the corresponding numerical computation of $\sum_{j=1}^{N_{ap}} \rho_j/\lambda_j^{2n+1}$, Eq. (18), with $N_{ap} = 1, 2, 5$.

TABLE 6

THE TOTAL POTENTIAL ENERGY $(-W)$ [a]

n	w^2	n	w^2
1	0.31426	6	0.38897
2	0.30973	7	0.42349
3	0.31856	8	0.46363
4	0.33615	9	0.50981
5	0.35983	10	0.56260

[a] Measured by taking $(\Upsilon^2 GL^2/R_e)$ as unity in Eq. (23) for different values of n.

We have computed both $\sigma_s^2(r)$ from Eq. (28) and $\sigma_p^2(R)$ from Eq. (24) for each value of n ($n = 1, 2, ..., 10$) with the Sérsic profile (see Figure 4). In all the cases we have calculated the corresponding mean quadratic velocity over the total space. We have found that $(\Upsilon GL/R_e)w^2 = 3\sigma_s^2$ and $\sigma_s^2 = \sigma_p^2$ with a precision greater that 0.01%, i.e., to at least four significant digits. This has been the precision that we have used in the calculation of the density, $\rho(r)$.

As we now have a "theoretical" distribution of $\sigma_p^2(R)$, we can compute the mean quadratic value, $\sigma_p^2(R_m)$, inside any total radius R_m and so we can evaluate the difference between the total and any partial integration. In Figure 5 we show the effects that can appear as a consequence of having a lack of data in the radial observational interval. We have calculated the mean quadratic partial value,

$$< \sigma_p^2(R_m) >= \frac{\int_0^{R_m} \sigma_p^2(R) \mathrm{d}L(R)}{\int_0^{R_m} \mathrm{d}L(R)}. \qquad (29)$$

Obviously, when $R_m \to \infty$ we find the total value $\sigma_p^2 = 1/3(\Upsilon GL/R_e)w^2$. But when R_m/R_e is too small we can find important differences between σ_p^2 and $\sigma_p^2(R_m)$, at least for some values of n of the Sérsic profile (see Fig. 5).

4. CONCLUSIONS

Once we admit that the distribution of the intensity over a galactocentric radius of a spherical galaxy can be well represented by the $R^{1/n}$ Sérsic profile a semi-analytical expression for the corresponding spatial density of luminous sources, $\rho_L(r)$, is given. It takes the form of a sum of exponentials with the same argument, $R^{1/n}$, as in the observed intensity profile, $I(R)$. But for $\rho_L(r)$ in each one of these exponentials, the argument $r^{1/n}$ is multiplied by a numerical factor, λ_j, and it is easily obtained. Likewise, the corresponding coefficient of each exponential is easily computed. The number (N_{ap}) of these exponentials (the order of approximation) depends on the required precision. A number between 5 and 10 can be sufficient for practical applications. Once this semi-analytical expression for the spatial density, $\rho(r)$, is found, the distribution of mass, $M(r)$, the potential, $\phi(r)$, and the velocity dispersions, $\sigma_s^2(r)$ and $\sigma_p^2(R)$, can be computed in a straightforward manner.

Furthermore, we show that the total mean quadratic of the measured velocity dispersion over the observational plane, $\sigma_p^2(R_m)$, cannot take the correct value σ_p^2 as a consequence of an incomplete integration because of lack of observations. The ratio between $\sigma_p^2(R_m)$ and σ_p^2 obtained by means of computations with parameters and the function of the "Sérsic" models provides us with the corresponding correction factor and, consequently, with the correct value of the velocity dispersion to use in the virial theorem to deduce the mass and mass-to-luminosity ratio.

We thank Terry Mahoney and Enrique Pérez for corrections to the manuscript. E. S. wants to thank the Instituto de Astronomía (UNAM) at Ensenada where part of this work was done.

REFERENCES

Abramowitz, M., & Stegun, I. A., 1964, Handbook of Mathematical Functions (New York: Dover)
Andreakis, Y. C., Peletier, R. F., & Balcells, M. 1995, MNRAS, 275, 874
Binggeli, B., & Jergen, H. 1998, A&A, 333, 17
Binney, J., & Tremaine, S. 1987, in Galactic Dynamics (Princeton: Princeton University Press)
Caon, N., Capaccioli, M., & D'Onofrio, M. 1993, MNRAS, 265, 1013
Ciotti, L. 1991, A&A, 249, 99
Davies, J. I., Phillips, S., Cawson, M. G. M., Disney, M. J., & Kibblewhite, E. J. 1988, MNRAS, 232, 239
de Vaucouleurs, G. 1948, Ann. d'Astroph., 11, 247
Gerbal, D., Lima Neto, G. B., Márquez, I., & Verhagen, H. 1997, MNRAS, 285, L41
Graham, A., Lauer, T. R., Colless, M., & Postman, M. 1996, ApJ, 465, 534
Graham, A., & Colless, M. 1997, MNRAS, 287, 221
Hubble, E. 1930, ApJ, 71, 231
Lindblad, B. 1956, Stockolms Obs. Ann., 19, n. 2
Mellier, Y., & Mathez, G. 1987, A&A, 175, 1
Poveda, A. 1958, Bol. Obs. Tonantzintla y Tacubaya, No. 17, 3
Poveda, A., Iturriaga, R., & Orozco, I. 1960, Bol. Obs. Tonantzintla y Tacubaya, No. 2, 20, p. 3
Reynolds, J.,H. 1913, MNRAS, 74, 132
Sérsic J. L. 1968, Atlas de Galaxias Australes (Córdoba: Observatorio Astronómico)
Stark, A. A. 1977, ApJ, 213, 368
Tricomi, F. G. 1985, Integral Equations (New York: Dover)
Young, P. J. 1976, AJ, 81, 807

Francisco Prada: Instituto de Astrofísica de Andalucía (CSIC), Camino Bajo de Húetor, 24, E-18008, Granada, Spain (fprada@iaa.es).
Eduardo Simonneau: Institut de Astrophysique, CNRS, 98bis, Bd. Arago, F-75014 Paris, France.